Journal of Medicinal Chemistry

Article

pubs.acs.org/jmc

Radiosynthesis and Evaluation of an ^{18}F-Labeled Positron Emission Tomography (PET) Radioligand for Brain Histamine Subtype-3 Receptors Based on a Nonimidazole 2-Aminoethylbenzofuran Chemotype

Xiaofeng Bao, Shuiyu Lu, Jeih-San Liow, Sami S. Zoghbi, Kimberly J. Jenko, David T. Clark, Robert L. Gladding, Robert B. Innis, and Victor W. Pike*

Molecular Imaging Branch, National Institute of Mental Health, National Institutes of Health, Building 10, Room B3 C346A, 10 Center Drive, Bethesda, Maryland, 20892, United States

Supporting Information

ABSTRACT: A known chemotype of H_3 receptor ligand was explored for development of a radioligand for imaging brain histamine subtype 3 (H_3) receptors in vivo with positron emission tomography (PET), namely nonimidazole 2-aminoethylbenzofurans, represented by the compound (*R*)-(2-(2-(2-methylpyrrolidin-1-yl)ethyl)benzofuran-5-yl)(4-fluorophenyl)-methanone (**9**). Compound **9** was labeled with fluorine-18 ($t_{1/2}$ = 109.7 min) in high specific activity by treating the prepared nitro analogue (**12**) with cyclotron-produced [^{18}F]-fluoride ion. [^{18}F]**9** was studied with PET in mouse and in monkey after intravenous injection. [^{18}F]**9** showed favorable properties as a candidate PET radioligand, including moderately high brain uptake with a high proportion of H_3 receptor-specific signal in the absence of radiodefluorination. The nitro compound **12** was found to have even higher H_3 receptor affinity, indicating the potential of this chemotype for the development of further promising PET radioligands.

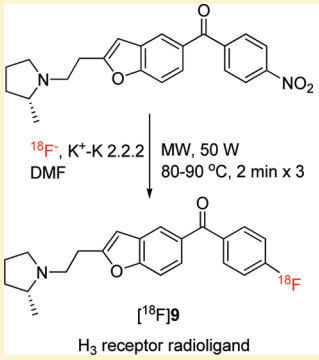

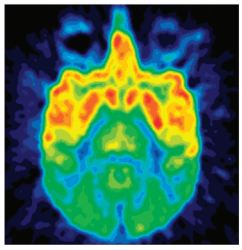
Axial PET image of monkey brain with [^{18}F]**9**

INTRODUCTION

The histamine subtype 3 (H_3) receptor is one of the four G-protein-coupled receptors of the histamine receptor family.[1−3] H_3 receptors are widely expressed in the mammalian brain and regulate the presynaptic release of histamine and other neurotransmitters such as acetylcholine, noradrenalin, and dopamine. Brain H_3 receptors are attractive drug targets for the treatment of cognitive and other disorders such as narcolepsy, attention-deficit hyperactivity disorder, and pain.[4,5]

The use of selective H_3 receptor radioligands with PET (positron emission tomography) has potential (i) to elucidate any changes in the distribution and density of H_3 receptors in living human brain during the progression of neuropsychiatric disorders, and (ii) to determine the dose-dependence of extent and duration of brain H_3 receptor occupancy by candidate drugs that may be directed at the treatment of such disorders.[6] So far, few radioligands have been prepared and evaluated for imaging brain H_3 receptors with PET. These radioligands may be structurally categorized as imidazoles, such as [^{18}F]FUB 272 ([^{18}F]**1**),[7] [^{18}F]VUF 5000 ([^{18}F]**2**),[8,9] [^{18}F]fluoroproxyfan ([^{18}F]**3**),[10,11] [^{11}C]UCL 1829 ([^{11}C]**4**),[7] or nonimidazoles, such as [^{11}C]JNJ-10181457 ([^{11}C]**5**),[12] [^{11}C]GSK189254 ([^{11}C]**6**),[13,14] [^{11}C]Merck 1b ([^{11}C]**7**),[15] and [^{18}F]Merck 2b ([^{18}F]**8**)[15] (Chart 1). The imidazoles have not shown encouraging results. Only the nonimidazoles [^{11}C]**6**, [^{11}C]**7**, and [^{18}F]**8** have shown promise in animal experiments, and only [^{11}C]**6** is known to have progressed to studies in human subjects.[14]

In our efforts to develop an ^{18}F-labeled H_3 receptor PET ligand, we selected a new chemotype, the reported nonimidazole 2-aminoethylbenzofuran-based H_3 receptor antagonist/inverse agonist **9**,[16] for radiolabeling and evaluation in animals. Ligand **9** appeared attractive as a candidate for development as a PET radioligand because it was already known to exhibit some of the properties recognized as being desirable,[17−20] including high affinity and selectivity for binding to target human receptors, ability to cross the blood−brain barrier, and potential to be labeled with no-carrier-added (NCA) fluorine-18 ($t_{1/2}$ = 109.7 min) at an aryl carbon.[21] Here we report the radiosynthesis of [^{18}F]**9** and an evaluation of its radioligand behavior in mouse and monkey. Our findings show [^{18}F]**9** is an effective H_3 receptor radioligand.

RESULTS AND DISCUSSION

Chemistry. Reference ligand **9** was prepared from commercially available (4-fluorophenyl)(4-hydroxyphenyl)-methanone, as described previously.[16] We prepared the nitro

Received: December 14, 2011
Published: February 7, 2012

Chart 1. Previously Reported PET Radioligands for H_3 Receptors (Imidazole-Based Radioligands Are Shown on the Left and Nonimidazole-Based Radioligands on the Right)

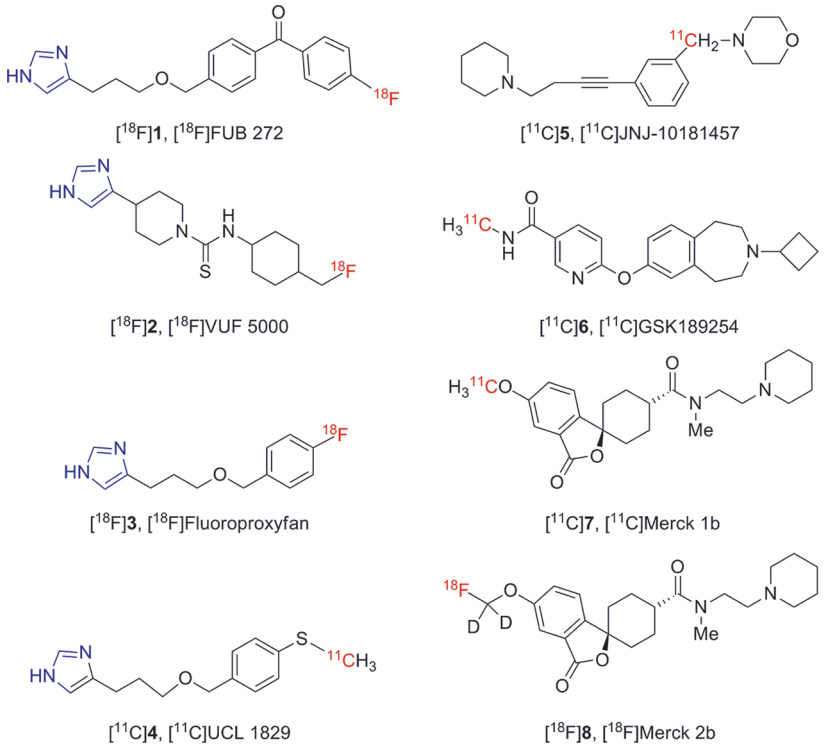

Scheme 1. Synthesis of Nitro Precursor 12[a]

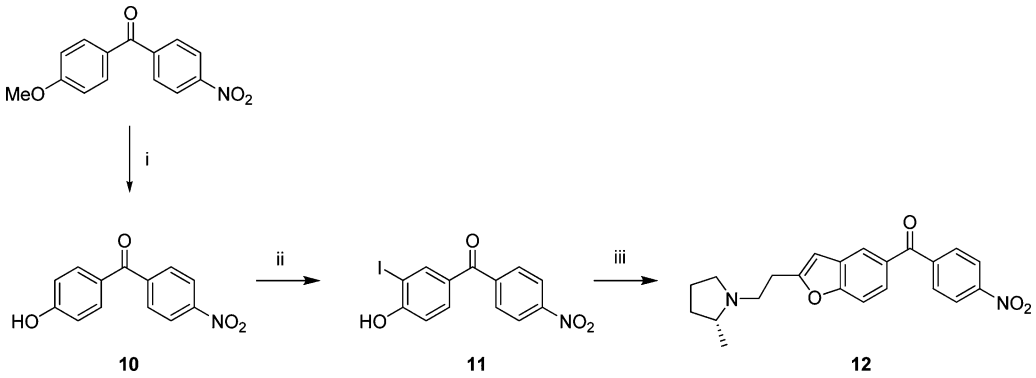

[a]Reagents, conditions and yields: (i) HBr, AcOH, reflux, 9 h; 87%; (ii) I_2, KI, NH_4OH, rt, 48 h; 26%; (iii) (a) 1-(3-butynyl)-2-(*R*)-methylpyrrolidine, $Pd(OAc)_2$, $(p\text{-tol})_3P$, CuI, rt, 10 min, (b) *i*-Pr_2NH, MeCN, 60 °C,16 h, 28%.

analogue **12** to provide a precursor suitable for use in a single-step labeling of **9** with cyclotron-produced NCA [^{18}F]fluoride ion because *p*-nitrophenylketones are well-known to be susceptible to aromatic nucleophilic substitution with [^{18}F]-fluoride ion.[21,22] The synthesis of **12** was analogous to that known[16] for the fluoro compound **9** (Scheme 1). An initial attempt to demethylate the commercially available (4-methoxyphenyl)(4-nitrophenyl)methanone with NaSMe in DMF[23,24] proved unsuccessful due to substitution of the nitro group to form a thioether. This observation nevertheless confirmed the susceptibility of the nitro group toward aromatic nucleophilic substitution. Selective demethylation of (4-methoxyphenyl)(4-nitrophenyl)methanone to the required (4-hydroxyphenyl)(4-nitrophenyl)methanone (**10**) was readily achieved by use of a non-nucleophilic Brønsted acid reagent, HBr in AcOH.[25,26] Treatment of **10** with 0.5 equiv of iodine and potassium iodide selectively produced **11** having iodine in ortho position to the hydroxy group in a moderate yield (30%) Use of a substoichiometric amount of iodine reduced the unwanted di-iodination that we observed from the use of a stoichiometric amount of iodine. 1-(3-Butynyl)-2(*R*)-methyl-pyrrolidine[16] was used directly as a MeCN solution (~0.1 M) for ring closure with **11** to give the target nitro precursor **12** in useful yield (28%).

Pharmacological Assays and Screening. Assay of compound **9** for binding to human recombinant H_3 receptors, expressed in HEK293T cells, confirmed high affinity with K_i in the nanomolar range (Table 1). The affinities of **9** for a wide range of other human recombinant receptors and binding sites, including the other subtypes of histamine receptor, were found to be at least 200-fold lower. These results accord with the previous report of the selectivity of **9** for binding to H_3

dx.doi.org/10.1021/jm201690h | *J. Med. Chem.* 2012, 55, 2406−2415

Table 1. K_i Values of Compounds 9 and 12 Determined from in Vitro Competitive Binding Assays

	K_i (nM)	
receptor or binding site	**9**	**12**
H_1	5440	7055
H_2	1708	923
H_3	1.9 ± 0.23	0.4 ± 0.04
H_4	>10000	>10000
5-HT_{1A}	432	>10000
5-HT_{1B}	>10000	>10000
5-HT_{1D}	6380	5237
5-HT_{2A}	2718	1355
5-HT_{2B}	3152	>10000
DAT	>10000	137
M_1	3266	931
M_2	462	681
M_3	204	512
M_4	351	415
M_5	437	336
all others[a]	>10000	>10000

[a] 5-$HT_{1E,2C,3,5A,6 \text{ and } 7}$, $\alpha_{1A,1B,1D,2A,2B \text{ and } 2C}$, β_{1-3}, D_{1-5}, $\sigma_{1,2}$, SERT, and NET

receptors among a wide battery of receptors (H_{1-4}, $D_{1,2s,2,4}$, 5-HT_{1-3}, adrenergic, and muscarinic) and transporters (NET, DAT, SERT) binding sites from unidentified species.[16] Therefore, **9** exhibited the necessary high human H_3 receptor affinity and selectivity for consideration as a candidate PET radioligand. The nitro precursor **12** was similarly screened and was found to have almost 5-fold higher affinity for human H_3 receptors and also greater than 200-fold selectivity for all other tested receptors and binding sites (Table 1).

Intrinsic activity may influence the utility of a PET radioligand for imaging G-protein coupled neuroreceptors. For example, antagonists are expected to bind to the full population of target receptors whether present in the G-protein coupled state or not, whereas agonists might be expected to bind only to the subpopulation of receptors in the G-protein coupled state. Ligand **9** was reported to be a competitive H_3 receptor antagonist in a variety of assays, including a Ca^{2+} flux assay, and also found to be a potent H_3 receptor inverse agonist for GTP-γ-S binding in H_3 receptor-transfected cells.[16] Both **9** and **12** were found to be inverse agonists in a GTP-γ-S assay performed by the Psychoactive Drug Screening Program.

Radiochemistry. [^{18}F]**9** was produced automatically within a lead-shielded hot-cell from cyclotron-produced [^{18}F]fluoride ion (200−300 mCi) in a Synthia device[27] equipped with a microwave heater (Scheme 2).[28] In trial experiments, reaction of **12** with [^{18}F]fluoride ion in DMF gave a higher decay-corrected radiochemical yield (RCY) of [^{18}F]**9** (34%) than in MeCN (2%) or in DMSO (6%). In these experiments, microwave power was set between 50 and 60 W so that reaction temperature did not exceed 90 °C because decomposition of [^{18}F]**9** became significant above 100 °C. [^{18}F]**9** was separated with single-pass reverse phase HPLC in high radiochemical purity (>99%). The pharmacologically active precursor **12** eluted at 29.1 min and was well separated from [^{18}F]**9** (t_R = 36.0 min). No residual **12** or other chemical impurity was detected in the formulated radioligand by analytical HPLC. The specific radioactivity of [^{18}F]**9**, when finally formulated for intravenous injection at about 110 min from the end of radionuclide production, was 1311 ± 221 mCi/μmol (n = 12). The average RCY of formulated [^{18}F]**9** was 9.3 ± 5.8% (n = 12).

Measurement of $LogD_{7.4}$ and Computation of cLogD and cLogP. The lipophilicity of a candidate radioligand is an important consideration[17−20,29,30] because this property strongly influences (i) ability of a radioligand to penetrate the blood−brain barrier, (ii) nonspecific binding of the radioligand in brain, (iii) the magnitude and measurability of the plasma free fraction (f_P), a parameter which may need to be known for the application of certain types of PET data quantitative analyses, and (iv) general susceptibility of a radioligand to metabolism. Moderate lipophilicity is usually considered desirable for achieving adequate blood−brain barrier penetration without incurring unacceptable nonspecific binding and for avoiding troublesome lipophilic brain-penetrant radiometabolites[29] and low f_P.[30] The measured $LogD_{7.4}$ of [^{18}F]**9** was 2.95 ± 0.06 (n = 6). Thus, the lipophilicity of **9** was found to be within the desirable range of LogD 1.5−3.5.[19] Computed cLogD (at pH = 7.4) values of **9** and **12** were 2.90 and 2.45, respectively, and hence Pallas software appears quite accurate for predicting lipophilicity for this type of structure. Computed LogP values for **9** and **12** were 4.79 ± 0.43 and 4.34 ± 0.34.

PET Imaging of [^{18}F]9 in Mice. Mouse brain is known to contain relatively (i) high densities of H_3 receptors in striatum, parietal cortex, insular cortex, nucleus acumbens, globus pallidus, and olfactory tubercle, (ii) moderate densities in thalamus, hypothalamus, and hippocampus, and (iii) low densities in cerebellum and brain stem.[31,32] H_3 receptor concentrations in striatum have been reported to be 95 fmol/mg tissue, which approximates to 95 nM.[31] A practical guideline[19] is that to achieve successful imaging with PET radioligands that are intended to bind reversibly to target receptors, B_{max}/K_d should exceed 10 in vivo. [^{18}F]**9** has a K_i value of 1.0 nM for rodent (rat) H_3 receptors[16] and therefore, the density of H_3 receptors (B_{max}, 95 nM) should be adequate for PET imaging with this radioligand.

Brain time−activity curves of [^{18}F]**9** in mice were acquired at baseline, and after treatment of mice with the selective high-affinity H_3 inverse agonist ciproxifan[33] (2.0 mg/kg, iv), nitro precursor **12** (2.0 mg/kg, iv), or ligand **9** itself (1.0 mg/kg, iv) (Figure 1). At baseline, radioactivity entered brain quickly after iv injection of [^{18}F]**9**, with peak whole brain uptake reaching a quite high level of 3.36 SUV at about 6.5 min. Brain radioactivity concentration then slowly declined to about 2.3 SUV by 90 min. In mice pretreated with ciproxifan, brain

Scheme 2. Radiosynthesis of [^{18}F]9

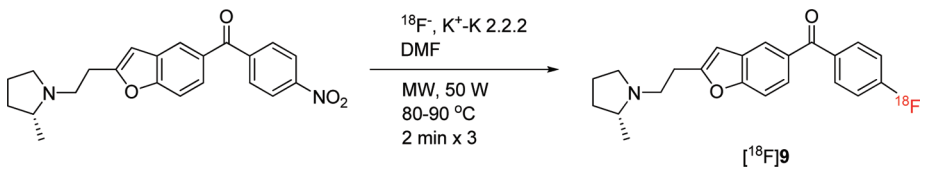

dx.doi.org/10.1021/jm201690h | J. Med. Chem. 2012, 55, 2406−2415

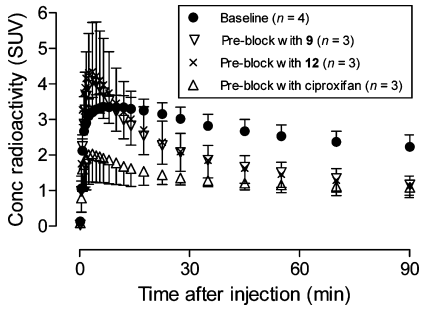

Figure 1. Whole brain time–activity curves after [^{18}F]**9** was injected in mice under baseline and pretreatment conditions. Data points are means with one-sided error bars showing SD.

radioactivity concentration quickly peaked at a lower level of about 1.98 SUV at 4.5 min after radioligand injection and then gradually reduced to 1.09 SUV at 90 min, a value much lower than seen at the same time after radioligand injection in the baseline experiment. When mice were pretreated with either the nitro precursor **12** or the ligand **9** itself, brain radioactivity peaked at 3.5 min and at higher values of 4.34 or 4.07 SUV, respectively. Brain radioactivity then decreased quickly to <1.20 SUV at 90 min, a level similar to that in the ciproxifan pretreatment experiment. Together, these data indicate that at baseline a high proportion of radioactivity in whole brain represents specific binding of [^{18}F]**9** to H_3-receptors.

The reasons for the differences in brain radioactivity uptake between the pretreatment experiments with ciproxifan and those using the structural congeners **12** and **9** are unclear. All three ligands appear to be highly selective for H_3 receptors. One possibility is that at their administered doses **12** and **9** displace the structurally similar [^{18}F]**9** from plasma proteins, giving a higher plasma free fraction (f_P) and greater entry of radioligand into brain than in the baseline experiment. Another possibility is that **12** or **9**, but not ciproxifan, blocks [^{18}F]**9** from binding to other unknown sites in periphery, thereby increasing availability of radioligand for brain entry. However, the cumulative in vitro data on the strong selectivity of both **12** and **9** for binding to H_3 receptors argue against this possibility. H_3 receptors also exist in peripheral organs such as lung and gastrointestinal tract.[1] The administered doses of the agents **9** and **12** may be more effective than that of ciproxifan at blocking the binding of [^{18}F]**9** to peripheral H_3 receptors, thereby increasing the free concentration of [^{18}F]**9** in plasma and hence uptake of radioactivity into brain. The imaging results, showing that [^{18}F]**9** gives a strong H_3-receptor specific signal in mice, encouraged our further evaluation of [^{18}F]**9** in nonhuman primate.

PET Imaging of [^{18}F]9 in Monkey. The distribution of H_3 receptors in rhesus monkey brain is similar to that in human brain.[15,34] As in rat, H_3 receptors are enriched in basal ganglia and also present in hippocampus and cortical areas, whereas cerebellum has lower levels of H_3 receptors.

Brain time–activity curves of [^{18}F]**9** in male rhesus monkey were acquired at baseline (Figure 2A) and after treatment with ciproxifan (2.0 mg/kg, iv) or **9** (1.0 mg/kg, iv) (Figure 2B). After injection of [^{18}F]**9** at baseline, radioactivity entered brain well with peak uptake in H_3 receptor-rich regions, such as striatum (4.45 SUV) and frontal cortex (3.86 SUV), occurring at about 27.5 and 47.5 min, respectively. Peak radioactivity concentration in other regions was lower but still higher than in cerebellum (2.76 SUV). The concentration of radioactivity in all regions slowly and continuously decreased to the end of the PET experiment (180 min).

Summed PET images of monkey brain at baseline showed a distribution of radioactivity reflecting the expected distribution of H_3 receptors (Figure 3), with no evidence of radioactivity uptake into skull.

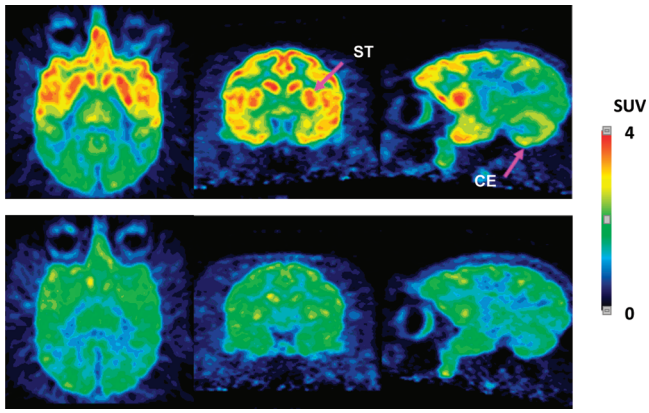

Figure 3. Axial, coronal, and sagittal PET images of brain through the striatum, after intravenous injection of a monkey with [^{18}F]**9** at baseline (top panel) and after treatment with **9** (1.0 mg/kg, iv) (bottom panel). Images were acquired for 180 min immediately after each radioligand injection.

Pretreatment of monkeys with ciproxifan reduced the peak radioactivity concentration in H_3 receptor-rich regions such as

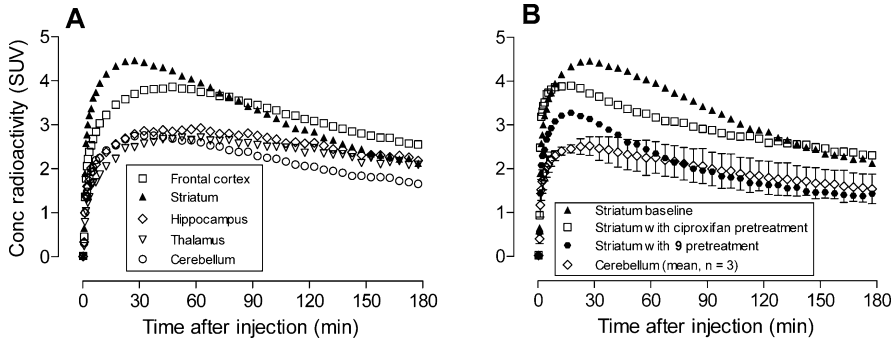

Figure 2. Brain region time–activity curves after [^{18}F]**9** was injected intravenously into monkey at baseline (A). (B) The effect of pretreatment with either ciproxifan (2.0 mg/kg, iv) or **9** (1 mg/kg, iv) on the time–activity curve for striatum. The mean curve for cerebellum from the three experiments is shown for comparison. Error bars represent mean ± SD.

dx.doi.org/10.1021/jm201690h | J. Med. Chem. 2012, 55, 2406–2415

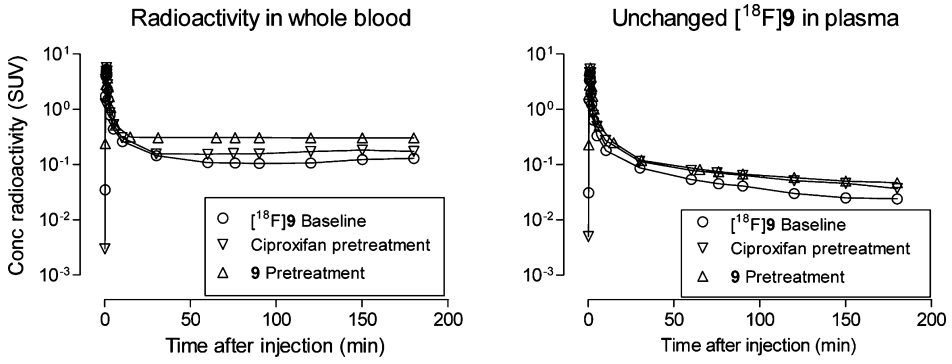

Figure 4. Time course of plasma concentration (SUV) of total radioactivity and unchanged [^{18}F]**9** after intravenous injection of [^{18}F]**9** into a rhesus monkey, under baseline, ciproxifan pretreatment, and **9**-pretreatment conditions..

frontal cortex and striatum but not in cerebellum. Subsequent washout of radioactivity from all H_3 receptor containing regions was slow. Pretreatment with **9** reduced peak radioactivity concentrations in all brain regions, and thereafter all brain region concentrations declined to a common low level at 180 min. The summed PET images from pretreatment experiments with **9** show a uniform low distribution of radioactivity across brain, again with no evidence of radioactivity uptake in skull. Thus, pretreatment with **9** appeared more effective than pretreatment with ciproxifan in showing specific binding of [^{18}F]**9** in monkey brain.

Ciproxifan is known to show species differences in H_3 binding affinity, with over 100-fold lower affinity for human H_3 receptors (K_i = 63 nM) than for rat H_3 receptors (K_i = 0.51 nM). The binding affinity of ciproxifan for monkey H_3 receptors is unknown. There is a possibility that the affinity of ciproxifan for monkey H_3 receptors is similar to that for human H_3 receptors, and this may account for incomplete blockade of the brain H_3 receptors at the administered dose.

Stability of [^{18}F]9 in Buffer, Whole Blood, and Plasma in Vitro. [^{18}F]**9** was found to be 98.8 ± 0.2% (n = 6) unchanged after 2.5 h in sodium phosphate buffer (pH 7.4) at room temperature and was also stable in monkey whole blood (98.4% ± 0.07%, n = 6) and monkey plasma (99.2% ± 0.1%, n = 6) at room temperature in vitro for 2.5 h. Therefore, accurate measurement of unchanged radioligand and radiometabolites in plasma was feasible by radio-HPLC for the ultimate purpose of generating radioligand arterial input functions.

Emergence of Radiometabolites of [^{18}F]9 in Monkey Plasma in Vivo. In the analyses of all studied monkey plasma samples, extractions of radioactivity from plasma with acetonitrile for radio-HPLC analysis were very effective (95.3 ± 7.44%, n = 115). After administration of [^{18}F]**9** into monkey at baseline, radioactivity cleared rapidly from plasma until about 50 min, when the low level of decay-corrected plasma radioactivity concentration became almost constant (Figure 4). Similar plasma time−radioactivity curves were seen in monkey that had been pretreated with ciproxifan or **9** (Figure 4). HPLC analyses of plasma showed that the concentration of unchanged radioligand declined continuously (Figure 4) while three radiometabolites [^{18}F]**A**−**C** emerged (Figure 5). These radiometabolites appeared to be less lipophilic than [^{18}F]**9** (t_R = 5.63 min) according to their shorter retention times on reverse phase HPLC (Figure 6). Radiometabolites emerged similarly in plasma of monkeys pretreated with ciproxifan (Figure 5). By contrast, in monkeys pretreated with **9**, parent radioligand more quickly decreased to become the minor component in plasma.

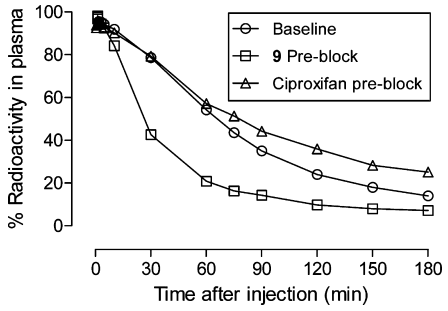

Figure 5. Percentage of radioactivity in plasma represented by unchanged radioligand after injection of a monkey with [^{18}F]**9** at baseline, after treatment with **9**, and after treatment with ciproxifan. The remainder of radioactivity was composed of radiometabolites [^{18}F]**A**−**C**.

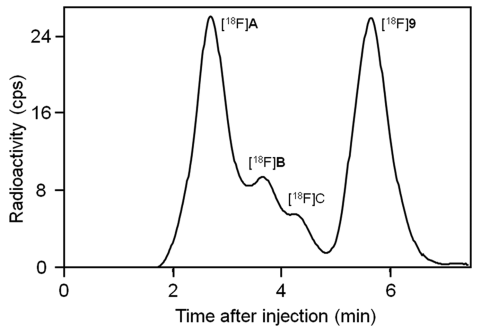

Figure 6. Reverse phase HPLC radiochromatogram of plasma sampled from monkey at 75 min after intravenous injection of [^{18}F]**9** (3.87 mCi). See text for details of analysis.

In these experiments, the least lipophilic radiometabolite [^{18}F]**A** became the major component in plasma. The ability of the radiometabolites to penetrate the blood−brain barrier is presently unknown. Nonetheless, because of their lower lipophilicities, these radiometabolites might be expected to enter brain less readily than parent radioligand. They would not therefore be expected to be troublesome to quantification of radioligand binding to H_3 receptors.

The routes of radioligand metabolism and the identities of the radiometabolites are also unknown. However, a close analogue of **9** having a nitrile (CN) group in place of the fluoro (F) group has been found to be a substrate for CYPs 3A4, 1A2, and 2D6 as well as flavin monooxygenases FMO-1 and FMO-3.[16] The lack of radioactivity uptake in skull (Figure 3) indicates that none of the radiometabolites of [^{18}F]**9** is

dx.doi.org/10.1021/jm201690h | J. Med. Chem. 2012, 55, 2406−2415

[^{18}F]fluoride ion and that radiodefluorination does not occur for this radioligand. Radioligands that radiodefluorinate may give high radioactivity uptake in skull which may compromise PET measurements in nearby brain through "partial volume effects".

Plasma Free Fraction of [^{18}F]9. The plasma free fraction (f_P) of [^{18}F]**9** in monkey plasma was accurately measurable and found to be 2.08 ± 0.14% at baseline and 1.4 ± 0.1% during pretreatment with **9**.

Biomathematical Analysis of PET Data Acquired with [^{18}F]9. Time−activity curves in baseline monkey experiments with [^{18}F]**9** fitted quite well to both one-tissue (1TC) and two-tissue (2TC) compartmental models. An *F* test showed that the 2TC model gave the best fit to acquired data (Figure 7).

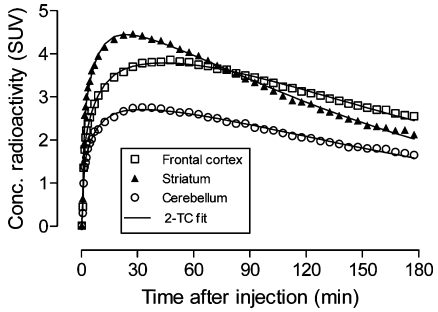

Figure 7. Fitting to two-tissue compartmental models of time−activity curves acquired in three brain regions after iv injection of monkey with [^{18}F]**9**.

Application of 2TC modeling of the data from the two monkeys showed that on average ciproxifan reduced the V_T 26−34% whereas **9** reduced V_T around 49−58% (Table 2). These data indicate that the majority of radioactivity in H_3 receptor-rich regions of brain represents specific binding of [^{18}F]**9** to H_3 receptors.

By truncating acquired PET data, we obtained V_T values for different time periods after radioligand injection. Reasonably stable V_T values were obtained from data acquired between 130 and 180 min (Figure 8), suggesting that for this radioligand in monkey, the ingress of troublesome radiometabolites into brain is not greatly problematic.

Comparison of [^{18}F]9 with Other H_3 Receptor Radioligands. The only other ^{18}F-labeled radioligand for brain H_3 receptors that has been reported to give a sizable receptor-specific signal in vivo is [^{18}F]**8** (Chart 1).[15] In rhesus monkey, this radioligand gives much lower peak brain radioactivity uptake (<1.3 SUV) in H_3 receptor-rich regions than [^{18}F]**9** (~4.5 SUV; Figure 2), although a somewhat higher proportion (~75%) of this lower radioactivity uptake appears to be receptor-specific binding. [^{18}F]**8** is labeled in a fluoromethoxy

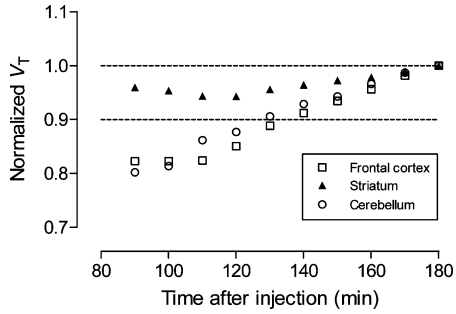

Figure 8. Time stability of normalized total volume of distribution (V_T) determined in three regions in one monkey with [^{18}F]**9**. Each V_T value was estimated from only the PET data collected up to that time point.

position which may be susceptible to radiodefluorination in human subjects in vivo to give high radioactivity uptake in bone including skull. Skull uptake of radioactivity is known to occur for other PET radioligands labeled with fluorine-18 in a fluoromethoxy position, including (*S,S*)-[^{18}F]FMeNER-d_2[35] and [^{18}F]FMEPEP-d_2.[36] In fact the incorporation of deuterium into these radioligands is intended to counter radiodefluorination in vivo. We found that [^{18}F]**9** shows no radiodefluorination in monkey. [^{18}F]**9** would not be expected to be radiodefluorinated in human subjects because aryl carbon−^{18}F bonds are usually stable in vivo. The radioligand [^{11}C]**7** has higher peak brain uptake (~2.3 SUV) than [^{18}F]**8**, but this is still lower than that of [^{18}F]**9**. However, [^{11}C]**7** appears superior in giving a very high proportion (~83%) of H_3 receptor-specific binding. The radioligand [^{11}C]**6** gave very high peak uptake in pig brain and a very high proportion (>90%) of H_3 receptor-specific signal.[13] So far, this is the only H_3 receptor radioligand studied in human subjects.[14] In baseline human experiments, this radioligand demonstrates progressively increasing radioactivity uptake in H_3 receptor-rich regions, apparently due to a slow off rate from the receptor. Although this high-affinity radioligand can be used to measure drug receptor occupancy, care has to be taken to avoid mass effects of coadministered carrier in the use of this radioligand, and in particular undesirably significant and prolonged occupancy of H_3 receptors by carrier.

CONCLUSIONS

[^{18}F]**9** demonstrates favorable properties as a PET radioligand for brain H_3 receptors in monkey, including moderately high brain uptake and sizable receptor-specific signal in the absence of radiodefluorination. Moreover, this study shows that higher affinity ligands, such as **12**, exist among this chemotype,[16] which may thus serve as a platform for developing further

Table 2. Estimation of V_T from 2TC Model in Two Monkeys Injected with [^{18}F]9 at Baseline, After Treatment with Ciproxifan, And after Treatment with 9

	monkey 1 V_t			monkey 2 V_t			mean V_t decrease (%)	
region	baseline	ciproxifan pretreatment	**9** pretreatment	baseline	ciproxifan pretreatment	**9** pretreatment	ciproxifan	**9** pretreatment
frontal cortex	64.1	43.5	29.5	42.1	26.7	16.4	−34	−58
striatum	54.7	42.7	29.1	45.3	31.6	19.7	−26	−52
hippocampus	60.4	45.3	31.2	50.8	30.4	20.8	−33	−54
thalamus	53.7	40.8	29.9	49.9	29.4	19.4	−33	−53
cerebellum	42.0	33.5	24.8	28.5	19.6	12.0	−26	−49

dx.doi.org/10.1021/jm201690h | *J. Med. Chem.* 2012, 55, 2406−2415

improved ^{11}C-labeled and ^{18}F-labeled H_3 receptor PET radioligands.

EXPERIMENTAL SECTION

Animal Procedures. All animal experiments were performed in accordance with the *Guide for Care and Use of Laboratory Animals*[37] and were approved by the National Institute of Mental Health Animal Care and Use Committee.

Materials and General Methods. All reagents and solvents were ACS grade or higher and used without further purification. Unless otherwise noted, all chemicals were purchased from Sigma-Aldrich (Milwaukee, WI). Reactions were performed under argon atmosphere with standard Schlenk techniques. 1-(3-Butynyl)-2-(*R*)-methylpyrrolidine was synthesized with a published method[16] from (*R*)-2-methylpyrrolidine and 3-butynyl-4-toluenesulfonate; this reagent was used as a ~0.1 M solution in MeCN without purification. Ligand **9** was prepared from commercially available (4-flourophenyl)(4-hydroxyphenyl)methanone, as described previously,[16] and obtained as a brown oil in >99% chemical purity.

^{1}H (400 MHz), ^{13}C NMR (100 MHz), and ^{19}F NMR (376 MHz) spectra were recorded on an Avance 400 spectrometer (Bruker; Billerica, MA). Chemical shifts are reported in δ units (ppm) downfield relative to the chemical shift for tetramethylsilane. Abbreviations br, s, d, t, and m denote broad, singlet, doublet, triplet, and multiplet, respectively. GC-MS spectra were obtained on a Polaris-Q GC-MS instrument (Thermo Fisher Scientific Corp., Waltham, MA). LC-MS was performed on a LCQ Deca instrument (Thermo Fisher Scientific Corp.) equipped with a reverse-phase HPLC column (Luna C18, 3 μm, 50 mm × 2 mm; Phenomenex, Torrance, CA), eluted at 200 μL/min with a mixture of A (H_2O−MeOH−AcOH, 90:10:0.5 v/v) and B (MeOH−AcOH, 100:0.5 v/v), initially composed of 20% B and linearly reaching 80% B in 3 min). High resolution mass spectra (HRMS) were acquired at the Mass Spectrometry Laboratory, University of Illinois at Urbana—Champaign (Urbana, IL) under electron ionization conditions with a double-focusing high resolution instrument (Autospec; Micromass Inc.). Thin layer chromatography was performed on silica gel layers (type 60 F254; EMD Chemicals, Gibbstown, NJ), and compounds were visualized under UV light (λ = 254 nm). Prepared compounds were analyzed by HPLC on a Prodigy column (10 μm, 4.6 mm × 250 mm; Phenomenex) eluted with 85%B at 2 mL/min with eluate monitored for absorbance at 243 nm (Gold 168 detector; Beckman) and were of >95% purity.

(4-Hydroxyphenyl)(4-nitrophenyl)methanone (10). (4-Methoxyphenyl)(4-nitrophenyl)methanone (150 mg, 0.58 mmol) was suspended in hydrobromic acid (5 mL, 48% w/w)[25,26] and glacial acetic acid (5 mL). The mixture was refluxed for 9 h and then taken to dryness under vacuum. The residue was dissolved in EtOAc and extracted with H_2O. The organic layer was dried with $MgSO_4$. After removal of solvent, flash chromatography (silica gel; EtOAc−hexane, 20:80, v/v) of the residue gave **10** as a gray solid (122 mg, 87%); mp 198−200 °C. ^{1}H NMR (CD_3OD): δ 8.24 (d, 2H, J = 8.8 Hz), 7.77 (d, 2H, J = 8.8 Hz), 7.62 (d, 2H, J = 8.8 Hz), 6.79 (d, 2H, J = 8.8 Hz). ^{13}C NMR (CD_3OD): δ 195.39, 164.44, 150.94, 145.42, 134.14, 131.38, 128.96, 124.50, 116.49 ppm. GC-MS: found 243.00 (M^+); calcd for $C_{13}H_9NO_4$, 243.05.

(4-Hydroxy-3-iodophenyl)(4-nitrophenyl)methanone (11). A solution of **10** (500 mg, 2.05 mmol) in NH_4OH (1 M, 17.1 mL) was stirred at 25 °C for 15 min and then treated with an aqueous solution (2.05 mL) of KI (1.69 g, 10.25 mmol) and I_2 (259 mg, 1.03 mmol) with stirring at 25 °C for 48 h. Solids were filtered off, dissolved in ethyl acetate, and then washed with H_2O and brine. The organic layer was dried with $MgSO_4$. After removal of solvent, flash chromatography (silica gel; EtOAc−hexane, 50:50 v/v) of the residue gave **11** as pale-yellow solid (190 mg, 26%); mp 248−250 °C. ^{1}H NMR (DMSO-d_6/CD_3OD): δ 8.31 (d, 2H, J = 8.4 Hz), 8.09 (s, 1H), 7.84 (d, 2H, J = 7.6 Hz), 7.62 (d, 1H, J = 8.4 Hz), 6.94 (d, 1H, J = 8.4 Hz). ^{13}C NMR (DMSO-d_6): δ 192.37, 162.25, 149.74, 143.75, 141.81, 133.00, 130.89, 129.48, 124.19, 115.03, 85.61 ppm. GC-MS: found 368.77 (M^+); calcd for $C_{13}H_8INO_4$, 368.95.

(*R*)-(2-(2-(2-Methylpyrrolidin-1-yl)ethyl)benzofuran-5-yl)(4-nitrophenyl)methanone (12). Compound **11** (0.500 g, 1.36 mmol) and a solution of 1-(3-butynyl)-2-(*R*)-methylpyrrolidine (0.1M) in MeCN (16.9 mL) were mixed in a round-bottomed flask (100-mL). $Pd(OAc)_2$ (9.0 mg, 0.04 mmol), tri-*p*-tolylphosphine (24.3 mg, 0.08 mmol), and CuI (77 mg, 0.40 mmol) were added. The resultant mixture was stirred at 25 °C for 10 min. *i*-Pr_2NH (1.9 mL, 13.6 mmol) was then added and the mixture heated at 60 °C for 16 h. The reaction mixture was allowed to cool and then filtered through a plug of Celite. The filtrate was concentrated under reduced pressure. Flash chromatography (silica gel; CH_2Cl_2−MeOH−NH_4OH, 90:9.9:0.1 by vol) of the residue gave **12** as a dark-brown semisolid (143 mg, 28%). ^{1}H NMR ($CDCl_3$): δ 8.35 (d, 2H, J = 6.8 Hz), 7.94 (m, 3H), 7.75 (d, 1H, J = 8.4 Hz), 7.53 (d, 1H, J = 8.4 Hz), 6.56 (s, 1H), 3.27 (m, 2H), 3.06 (t, 2H, J = 8.4 Hz), 2.54 (m, 1H), 2.44 (m, 1H), 2.26 (m, 1H), 1.98 (m, 1H), 1.80 (m, 2H), 1.48 (m, 1H), 1.16 (d, 3H, J = 6.0 Hz) ppm. ^{13}C NMR ($CDCl_3$): δ 194.61, 159.80, 157.43, 149.54, 143.77, 131.25, 130.55, 129.09, 125.97, 123.68, 123.44, 111.08, 103.14, 60.34, 53.76, 51.60, 32.58, 27.90, 21.66, 18.70 ppm. LC-MS (M^+ + 1) 379.1. HRMS (M^+ + 1) found, 379.1668; calcd for $C_{22}H_{23}N_2O_4$, 379.1658. HPLC: t_R = 12.7 min, purity >99%.

Production of NCA [^{18}F]fluoride Ion Reagent. NCA [^{18}F]-fluoride ion was produced by irradiating ^{18}O-enriched water (98 atom %) with a beam (20 μA) of 16.5 MeV protons[38] from a PETrace cyclotron (GE, Uppsala, Sweden) for 120 min. At the end of irradiation, the aqueous solution (20−200 μL) of [^{18}F]fluoride ion (20−200 mCi) was transferred in a glass V-vial (1 mL) to a lead-shielded hot-cell and placed in the cavity of a model 521 instrument for accelerated microwave chemistry (Resonance Instruments Inc., Skokie, IL). The latter is integrated with a Synthia MKII radiochemistry platform inside the same hot-cell, as described previously.[28] A solution of K_2CO_3/K 2.2.2 (100 μL stock solution of 0.5 mg K_2CO_3 and 5.0 mg K 2.2.2 in 9:1 MeCN and H_2O mixture) and MeCN (600 μL) were added to the V-vial, which was then placed under N_2 gas flow (200 mL/min) and irradiated with microwaves (90 W in 2 × 2 min pulses). The addition of acetonitrile (600 μL) followed by microwave irradiation was repeated three times to give dry NCA [^{18}F]fluoride ion-K^+−K 2.2.2 reagent.

Radiosynthesis of [^{18}F]9. Precursor **12** (1.0 mg) in DMF (0.3 mL) was introduced into the vial containing anhydrous [^{18}F]fluoride ion-K^+−K 2.2.2 and irradiated with microwaves (50−55 W) in 3 × 2 min pulses. The reaction temperature was carefully held between 80 and 90 °C during the irradiation. The reaction mixture was then diluted with water (0.7 mL) and injected onto a reverse phase column (Prodigy, 10 μm, 10 mm × 250 mm; Phenomenex) eluted at 6 mL/min with a mixture of aq NH_4OH (0.025%, pH 8.5) (A, 70%) and MeCN (B, 30%). B was kept at 30% for 5 min, linearly increased to 70% over 3 min, and then held at 70% for 45 min. The collected fraction of [^{18}F]**9** (t_R, 34−36 min) was transferred to a pear-shaped flask and the solvent removed under vacuum. The residue was diluted with sterile saline for injection (10 mL) containing EtOH (10%; USP grade) and passed through a sterile filter (2.5 μm, Millex MP, Millipore, Bedford, MA). The pH of the final dose was in the range 6−8.

RCY was calculated from the radioactivity of formulated [^{18}F]**9**. Chemical and radiochemical purities, and specific radioactivity were determined by reverse phase HPLC on a Prodigy column (10 μm, 4.6 mm × 250 mm; Phenomenex) eluted with 20% A and 80%B at 2 mL/min with eluate monitored for absorbance at 243 nm (Gold 166 detector, Beckman) and for radioactivity (PMT, HC-003; Bioscan Inc., Washington, DC). [^{18}F]**9** (t_R = 17.9 min) was identified by, (i) coelution with nonradioactive **9** in the aforementioned analytical HPLC method, and (ii) LC-MS analysis of associated carrier for comparison with that of ref 9 (m/z = 352 (M^+ + 1)).

Computation of cLogP and cLogD and Measurement of LogD. cLogP and cLogD (at pH = 7.4) values for **9** were computed with the program Pallas 3.0 for Windows (CompuDrug; San Francisco, CA). The LogD value of [^{18}F]**9** was measured as the log

of its distribution coefficient between *n*-octanol and sodium phosphate buffer (0.15 M, pH 7.4), as described previously.[39,40] [^{18}F]**9** was shown to be stable to buffer by radio-HPLC analysis. The radioactivity in the organic phase and that in the aqueous phase were counted in a γ-counter. Counting errors were <0.3 ± 0.1% (n = 6) at one standard deviation.

PET Imaging of [^{18}F]9 in Mouse. Wild type FVB mice (Taconic Farm, Germantown, NY) were anesthetized with 1.5% isoflurane in oxygen, and body temperatures were maintained at 36.5−37.0 °C with a heating lamp. Intravenous injections were performed via polyethylene cannulae (PE-10; Becton Dickinson, Franklin Lakes, NJ) in the tail vein. The cannulae were secured with tissue adhesive (Vetbond; 3M, St. Paul, MN). Thirteen mice (27.6 ± 3.8 g) were scanned either at baseline (n = 4) or after treatment with ciproxifan (2.0 mg/kg, iv; n = 3), **9** (1.0 mg/kg, iv; n = 3), or **12** (1.0 mg/kg, iv; n = 3) 30 min before injection of [^{18}F]**9**.

Serial dynamic scans were acquired with a Focus 120 microPET scanner (Siemens Medical Solutions, Knoxville, TN) started at the time of injection of NCA [^{18}F]**9** (73 ± 29 μCi) and were continued for 120 min with increasing frame durations from 20 s to 20 min. Images were reconstructed by a Fourier rebinning/2D ordered-subset expectation maximization algorithm. No attenuation or scatter correction was applied. Whole brain decay-corrected time−activity curves were generated using PMOD 3.0 (PMOD Technologies, Zurich, Switzerland). Brain uptake of radioactivity was expressed as standardized uptake value (SUV) where SUV = (% injected dose per cm^3 brain) × (g body weight).

PET Imaging of [^{18}F]9 in Monkey. Four male rhesus monkeys (7.3 ± 0.8 kg) were used for PET scans of the brain. Two of the monkeys had femoral artery indwelling catheters for blood sampling. All four monkeys were studied at baseline (n = 4), three at 30 min after treatment with ciproxifan (2.0 mg/kg, iv) and two at 30 min after treatment with **9** (1.0 mg/kg, iv). All monkeys were immobilized with ketamine (10 mg/kg, im) and maintained in anesthesia with 1.5% isoflurane in O_2 via an endotracheal tube. NCA [^{18}F]**9** (3.91 ± 0.46 mCi, n = 9) was injected intravenously. All PET scans were acquired with a Focus 220 microPET scanner (Siemens Medical Solutions, Knoxville, TN) for 180 min except one scan for 120 min. Each scan consisted of 45 frames of increasing duration, from 30 s to 5 min. Images were reconstructed with a Fourier rebinning/2D filtered back projection algorithm with scatter and attenuation correction. All data were decay-corrected to the time of radioligand injection.

With a view to analyzing monkey plasma for radiometabolites and thereby measuring an arterial-input function of unchanged radioligand, the stability of [^{18}F]**9** for 2.5 h in whole monkey blood and plasma in vitro was first confirmed by the radio-HPLC method to be used for radiometabolite analysis. This method used a reverse phase column (Novapak C18, 4 μm, 100 mm × 8 mm; Waters Corp.) within a radial compression module (RCM-100) that was eluted at 2.0 mL/min with MeOH−H_2O−Et_3N (85:15:0.1 by vol). Upon radioligand injection in each of the PET scans in two of the monkeys, arterial blood was sampled into heparin-treated syringes at every 15 s for 2 min, followed by further sampling at 3, 5, 10, 30, 60, 75, 90, 120, 150, and 180 min from injection. Plasma [^{18}F]**9** was then quantified in each sample with radio-HPLC, as previously described.[41]

The time course of the plasma concentration of [^{18}F]**9** separated from radiometabolites was used as the input function for compartmental analysis. The total concentration of radioactivity in whole blood was used for vascular correction of the PET data, assuming that blood constitutes 5% of brain volume. The free fraction (f_P) of [^{18}F]**9** in plasma was measured by ultrafiltration, as described previously.[42] Measurements on each plasma sample were made in triplicate.

All monkey images were spatially normalized to a standardized template[43] using a mutual information algorithm (FSL Library, Oxford, UK). Time−activity curves were generated by applying a set of 34 predefined region-of-interests on the template. The concentration of radioactivity in each region was expressed as SUV. Time−activity curves were fitted to one and two tissue compartmental models. The two-tissue compartment model was applied to calculate the total distribution volume (V_T) under the three different conditions (baseline, ciproxifan pretreatment, and **9** pretreatment). Time−activity curve generation and nonlinear parameter fitting was carried out with PMOD 3.0.

■ ASSOCIATED CONTENT

Ⓢ Supporting Information

Chromatograms for the separation and analysis of [^{18}F]**9**. This material is available free of charge via the Internet at http://pubs.acs.org.

■ AUTHOR INFORMATION

Corresponding Author

*Phone: (301) 594 5986. Fax: (301) 480 5112. E-mail: pikev@mail.nih.gov.

Notes

The authors declare no competing financial interest.

■ ACKNOWLEDGMENTS

This study was supported by the Intramural Research Program of the National Institutes of Health (NIMH). We thank the NIH Clinical PET Department (Chief Dr. P. Herscovitch) for fluorine-18 production and PMOD Technologies for providing the image analysis software. Receptor binding assays were performed by the National Institute of Mental Health's Psychoactive Drug Screening Program, contract no. HHSN-271-2008-00025-C (NIMH PDSP). The NIMH PDSP is directed by Dr. Bryan L. Roth, MD Ph.D., at the University of North Carolina at Chapel Hill and Project Officer Jamie Driscoll at NIMH, Bethesda, MD, USA. We also thank Cheryl L. Morse (NIMH) for assistance in radiochemistry.

■ ABBREVIATIONS USED

5-HT, serotonin; DAT, dopamine transporter; DMF, *N*,*N*-dimethylformamide; DMSO, dimethyl sulfoxide; f_P, plasma free fraction; GTP, guanosine triphosphate; H_3, histamine subtype-3; HPLC, high performance liquid chromatography; HRMS, high resolution mass spectrometry; NCA, no-carrier-added; NET, noradrenalin transporter; PET, positron emission tomography; RCY, decay-corrected radiochemical yield; SERT, serotonin transporter; SUV, standardized uptake value

■ REFERENCES

(1) Schwartz, J. C.; Arrang, J. M.; Garbarg, M.; Pollard, H. A third histamine receptor subtype: characterisation, localisation and functions of the H_3 receptor. *Agents Actions* **1990**, *30*, 13−23.

(2) Cumming, P.; Shaw, C.; Vincent, S. R. High affinity histamine binding site is the H_3 receptor: characterization and autoradiographic localization in rat brain. *Synapse* **1991**, *8*, 144−151.

(3) Pillot, C.; Heron, A.; Cochois, V.; Tardivel-Lacombe, J.; Ligneau, X.; Schwartz, J. C.; Arrang, J.-M. A detailed mapping of the histamine H_3 receptor and its gene transcripts in rat brain. *Neuroscience* **2002**, *114*, 173−193.

(4) Leurs, R.; Bakker, R. A.; Timmerman, H.; de Esch, I. J. P. The histamine H_3 receptor: from gene cloning to H_3 receptor drugs. *Nature Rev. Drug Discovery* **2005**, *4*, 107−120.

(5) Berlin, M.; Boyce, C. W.; de Lera Ruiz, M. Histamine H_3 receptor as a drug target. *J. Med. Chem.* **2011**, *54*, 26−53.

(6) Yanai, K.; Tashiro, M. The physiological and pathophysiological roles of neuronal histamine: an insight from human positron emission tomography studies. *Pharmacol. Ther.* **2007**, *113*, 1−15.

(7) Ponchant, M.; Demphel, S.; Fuseau, C.; Coulomb, C.; Bottlaender, M.; Schwartz, J. C.; Stark, H.; Schunack, W.; Athmani, S.; Ganellin, R.; Crouzel, C. Radiosynthesis and biodistribution of two

potential antagonists of cerebral histamine H_3 receptors for PET studies: [^{18}F]FUB 272 and [^{11}C]UCL 1829. *J. Labelled Compd. Radiopharm.* **1997**, *40*, 605−607.
(8) Windhorst, A. D.; Timmerman, H.; Menge, W. M. P. B; Leurs, R.; Herscheid, J. D. M. Synthesis, in vitro pharmacology and radiosynthesis of *N*-(*cis*-4-fluoromethylcyclohexyl)-4-(1(*H*)-imidazol-4-yl)piperidine-1-thiocarbonamide (VUF 5000), a potential PET ligand for the histamine H_3 receptor. *J. Labelled Compd. Radiopharm.* **1999**, *42*, 293−307.
(9) Windhorst, A. D.; Timmerman, H.; Klok, R. P.; Menge, W. M. P. B; Leurs, R.; Herscheid, J. D. M. Evaluation of [^{18}F]VUF 5000 as a potential PET ligand for brain imaging of the histamine H_3 receptor. *Bioorg. Med. Chem.* **1999**, *7*, 1761−1767.
(10) Iwata, R.; Horvath, G.; Pascali, C.; Bogni, A.; Yanai, K.; Kovacs, Z.; Ido, T. Synthesis of 3-[1*H*-imidazol-4-yl]propyl 4-[^{18}F]-fluorobenzyl ether ([^{18}F]fluoroproxyfan): a potential radioligand for imaging histamine H_3 receptors. *J. Labelled Compd. Radiopharm.* **2000**, *43*, 873−882.
(11) Funaki, Y.; Sato, K.; Kato, M.; Ishikawa, Y.; Iwata, R.; Yanai, K. Evaluation of the binding characteristics of [^{18}F]fluoroproxyfan in the rat brain for in vivo visualization of histamine H_3 receptor. *Nucl. Med. Biol.* **2007**, *34*, 981−987.
(12) Airaksinen, A. J.; Jablonowski, J. A.; van der Mey, M.; Barbier, A. J.; Klok, R. P.; Verbeek, J.; Schuit, R.; Herscheid, J. D. M.; Leysen, J. E.; Carruthers, N. I.; Lammertsma, A. A.; Windhorst, A. D. Radiosynthesis and biodistribution of a histamine H_3 receptor antagonist 4([3-(4-piperidin-1-nyl-but-1-ynyl)-[^{11}C]benzyl]-morpholine: evaluation of a potential PET radioligand. *Nucl. Med. Biol.* **2006**, *33*, 801−810.
(13) Plisson, C.; Gunn, R. N.; Cunningham, V. J.; Bender, D.; Salinas, C. A.; Medhurst, A. D.; Roberts, J. C.; Laruelle, M.; Gee, A. D. ^{11}C-GSK189254: a selective radioligand for in vivo central nervous system imaging of H_3 receptors by PET. *J. Nucl. Med.* **2009**, *50*, 2064−2072.
(14) Ashworth, S.; Rabiner, E. A.; Gunn, R. N.; Plisson, C.; Wilson, A. A.; Comley, R. A.; Lai, R. Y. K.; Gee, A. D.; Laruelle, M.; Cunningham, V. J. Evaluation of ^{11}C-GSK189254 as a novel radioligand for the H_3 receptor in humans using PET. *J. Nucl. Med.* **2010**, *51*, 1021−1029.
(15) Hamill, T. G.; Sato, N.; Jitsuoka, M.; Tokita, S.; Sanabria, S.; Eng, W.; Ryan, C.; Krause, S.; Takenaga, N.; Patel., S.; Zeng, Z.; Williams, D. Jr.; Sur, C.; Hargreaves, R.; Burns, H. D. Inverse agonist histamine H_3 receptor PET tracers labelled with carbon-11 or fluorine-18. *Synapse* **2009**, *63*, 1122−1132.
(16) Cowart, M.; Faghih, R.; Curtis, M. P.; Gfesser, G. A.; Bennani, Y. L.; Black, L A.; Pan, L.; Marsh, K. C.; Sullivan, J. P.; Esbenshade, T. A.; Fox, G. B.; Hancock, A. A. 4-(2[2-(2(*R*)-Methylpyrrolidin-1-yl)ethyl]benzofuran-5-yl)benzonitrile and related 2-aminoethylbenzofuran H_3 receptor antagonists potently enhance cognition and attention. *J. Med. Chem.* **2005**, *48*, 38−55.
(17) Pike, V. W. Positron-emitting radioligands for studies in vivo—probes for human psychopharmacology. *J. Psychopharmacology* **1993**, *7*, 139−158.
(18) Laruelle, M.; Slifstein, M.; Huang, Y. Relationships between radiotracer properties and image quality in molecular imaging of the brain with positron emission tomography. *Mol. Imaging Biol.* **2003**, *5*, 363−375.
(19) Patel, S.; Gibson, R. In vivo site-directed radiotracers: a mini-review. *Nucl. Med. Biol.* **2008**, *35*, 805−815.
(20) Pike, V. W. PET Radiotracers: crossing the blood−brain barrier and surviving metabolism. *Trends Pharmacol. Sci.* **2009**, *30*, 431−440.
(21) Cai, L.; Lu, S.; Pike, V. W. Chemistry with [^{18}F]fluoride ion. *Eur. J. Org. Chem.* **2008**, *17*, 2853−2873.
(22) Attina, M.; Cacace, F.; Wolf, A. P. Labeled aryl fluorides from the nucleophilic displacement of activated nitro groups by ^{18}F−F$^-$. *J. Labelled Compd. Radiopharm.* **1983**, *20*, 501−514.
(23) Feutrill, G. I.; Mirrington, R. N. Demethylation of aryl methyl ethers with thioethoxide ion in dimethyl formamide. *Tetrahedron Lett.* **1970**, 1327−1328.
(24) Kubo, K.; Ohyama, S.; Shimizu, T.; Takami, A.; Murooka, H.; Nishitoba, T.; Kato, S.; Yagi, M.; Kobayashi, Y.; Iinuma, N.; Isoe, T.; Nakamura, K.; Iijima, H.; Osawa, T.; Izawa, T. Synthesis and structure−activity relationship for new series of 4-phenoxyquinoline derivatives as specific inhibitors of platelet-derived growth factor receptor tyrosine kinase. *Bioorg. Med. Chem.* **2003**, *11*, 5117−5133.
(25) Surrey, A. R. Pyrocyanine. *Org. Synth. Collected Vol.* **1955**, *3*, 753; *Org. Synth.* **1946**, *26*, 86−90.
(26) Kawasaki, I.; Matsuda, K.; Kaneko, T. Preparation of 1,7-bis(*p*-hydroxyphenyl)heptane. *Bull. Chem. Soc. Jpn.* **1971**, *44*, 1986−1987.
(27) Bjurling, P.; Reineck, R.; Westerberg, G.; Gee, A. D.; Sutcliffe, J.; Långström, B. *Proceedings of the VIth Workshop on Targetry and Target Chemistry*; TRIUMF: Vancouver, Canada, 1995; pp 282−284.
(28) Lazarova, N.; Siméon, F. G.; Musachio, J. L.; Lu, S.; Pike, V. W. Integration of a microwave reactor with Synthia to provide a fully automated radiofluorination module. *J. Labelled Compd. Radiopharm.* **2007**, *50*, 463−465.
(29) Waterhouse, R. N. Determination of lipophilicity and its use as a predictor of blood−brain barrier penetration of molecular imaging agents. *Mol. Imaging Biol.* **2003**, *5*, 376−389.
(30) Zoghbi, S. S.; Anderson, K. B.; Jenko, K. J.; Luckenbaugh, D. A.; Innis, R. B.; Pike, V. W. On quantitative relationships between drug-like compound lipophilicity and plasma free fraction in monkey and human. *J. Pharm. Sci.* **2012**, *101*, 1028−1039.
(31) Cumming, P.; Laliberté, C.; Gjedde, A. Distribution of histamine H_3 binding in forebrain of mouse and guinea pig. *Brain Res.* **1994**, *664*, 276−279.
(32) Jansen, F. P.; Mochizuki, T.; Maeyama, K.; Leurs, R.; Timmerman, H. Characterization of histamine H_3 receptors in mouse brain using the H_3 antagonist [^{125}I]iodophenpropit. *Naunyn-Schmiedeberg's Arch. Pharmacol.* **2000**, *362*, 60−67.
(33) Ligneau, X.; Lin, J.-S.; Vanni-Mercier, G.; Jouvet, M.; Muir, J. L.; Ganellin, C. R.; Stark, H.; Elz, S.; Schunack, W.; Schwartz, J.-C. Neurochemcial and behavioral effects of ciproxifan, a potent histamine H_3-receptor antagonist. *J. Pharmacol. Exp. Ther.* **1998**, *287*, 658−666.
(34) Martinez-Mir, M. I.; Pollard, H.; Moreau, J.; Arrang, J. M.; Ruat, M.; Traiffort, E.; Schwartz, J. C.; Palacios, J. M. Three histamine receptors (H1, H2 and H3) visualized in the brain of human and non-human primates. *Brain Res.* **1990**, *526*, 322−327.
(35) Takano, A.; Halldin, C.; Varrone, A.; Karlsson, P.; Sjöholm, N.; Stubbs, J. B.; Schou, M.; Airaksinen, A. J.; Tauscher, J.; Gulyas, B. Biodistribution and radiation dosimetry of the norepinephrine transporter radioligand (*S*,*S*)-[^{18}F]FMeNER-D$_2$: a human whole-body PET study. *Eur. J. Nucl. Med. Mol. Imaging* **2008**, *35*, 630−636.
(36) Terry, G. E.; Hirvonen, J.; Liow, J.-S.; Zoghbi, S. S.; Gladding, R.; Tauscher, J. T.; Schaus, J. M.; Phebus, L.; Felder, C. C.; Morse, C. L.; Donohue, S. R.; Pike, V. W.; Halldin, C.; Innis, R. B. Imaging and quantitation of cannabinoid CB$_1$ receptors in human and monkey brains using ^{18}F-labeled inverse agonist radioligands. *J. Nucl. Med.* **2010**, *51*, 112−120.
(37) Clark, J. D.; Baldwin, R. L.; Bayne, K. A.; Brown, M. J.; Gebhart, G. F.; Gonder, J. C.; Gwathmey, J. K.; Keeling, M. E.; Kohn, D. F.; Robb, J. W.; Smith, O. A.; Steggerda, J.-A. D.; VandeBer, J. L. *Guide for the Care and Use of Laboratory Animals*; National Academy Press: Washington DC, 1996.
(38) Guillaume, M.; Luxen, A.; Nebeling, R.; Argentini, M.; Clark, J. C.; Pike, V. W. Recommendations for fluorine-18 production. *Appl. Radiat. Isot.* **1991**, *42*, 749−762.
(39) Zoghbi, S. S.; Baldwin, R. M.; Seibyl, J. P.; Charney, D. S.; Innis, R. B. A radiotracer technique for determining apparent pK_a of receptor binding ligands. *J. Labelled Compd. Radiopharm.* **1997**, *40* (S1), 136−138.
(40) Briard, E.; Zoghbi, S. S.; Imaizumi, M.; Gourley, J. P.; Shetty, H. U.; Hong, J.; Cropley, V.; Fujita, M.; Innis, R. B.; Pike, V. W. Synthesis and evaluation in monkey of two sensitive ^{11}C-labeled aryloxyanilide ligands for imaging brain peripheral benzodiazepine receptors in vivo. *J. Med. Chem.* **2008**, *51*, 17−30.
(41) Zoghbi, S. S.; Shetty, H. U.; Ichise, M.; Fujita, M.; Imaizumi, M.; Liow, J. S.; Shah, J.; Musachio, J. L.; Pike, V. W.; Innis, R. B. PET

imaging of the dopamine transporter with [^{18}F]FECNT: a polar radiometabolite confounds brain radioligand measurements. *J. Nucl. Med.* **2006**, *47*, 520−527.
(42) Gandelman, M. S.; Baldwin, R. M.; Zoghbi, S. S.; Zea-Ponce, Y.; Innis, R. B. Evaluation of ultrafiltration for the free-fraction determination of single photon emission computed tomography (SPECT) radiotracers: *β*-CIT, IBF, and iomazenil. *J. Pharm. Sci.* **1994**, *83*, 1014−1019.
(43) Yasuno, F.; Brown, A. K.; Zoghbi, S. S.; Krushinski, J. H.; Chernet, E.; Tauscher, J.; Schaus, J. M.; Phebus, L. A.; Chesterfield, A. K.; Felder, C. C.; Gladding, R. L.; Hong, J.; Halldin, C.; Pike, V. W.; Innis, R. B. The PET radioligand [^{11}C]MePPEP binds reversibly and with high specific signal to cannabinoid CB_1 receptors in nonhuman primate brain. *Neuropsychopharmacology* **2008**, *33*, 259−269.